JOURNAL OF COMPUTATIONAL PHYSICS 41, 167–191 (1981)

Finite Element Simulations of Steady, Two-Dimensional, Viscous Incompressible Flow over a Step*

JOHN M. LEONE, JR.,† AND PHILIP M. GRESHO

Lawrence Livermore Laboratory, University of California, Livermore, California 94550

Received July 25, 1979; revised January 29, 1980

The Galerkin finite element method is utilized to obtain quite detailed results for flow through a channel containing a step at Reynolds numbers of 0 and 200. This technique, however, like its centered finite difference counterpart, is prone to generating wiggles or oscillations when streamwise gradients become too large to be resolved by the mesh. These wiggles are carefully analyzed and are used as a guide in obtaining accurate solutions via successive mesh refinement. It is argued that the appropriate solution to the wiggle problem is the utilization of selective grid refinement (easily available via isoparametric finite elements) rather than taking recourse to upwind methods which effectively reduce the local Reynolds number and thereby generate deceptively smooth and often inaccurate results.

INTRODUCTION

Inspired and challenged by the recent work of Hughes *et al.* [1], wherein they essentially recommend the abandonment of conventional Galerkin methods for the finite element discretization of the Navier–Stokes equations in favor of an ad hoc, modified approach ("optimal upwinding") which ostensibly yields a "solution" (and eliminates spurious "wiggles") for any Reynolds number (Re), we embarked upon this study with the goal of shedding more light on the following relevant and important question: "Can one obtain smooth and accurate solutions without resolving the boundary layer?" (See also Hedstrom and Osterheld [2], who address somewhat similar issues, both analytically and via finite difference calculations.)

Since we needed to address a number of related issues along the way, such as grid resolution, boundary conditions, and mathematical singularities, we have decided to present our results somewhat in the manner of a "case study"; many of our observations for this particular simulation will apply to other flows and may therefore be useful to others. The presentation is developed along the following lines: (1) statement of the problem, (2) a very brief review of previous work, (3) presentation of our results for Stokes flow ($Re = 0$) and for $Re = 200$ using various domain

* Work performed under the auspices of the U. S. Department of Energy by Lawrence Livermore Laboratory under Contract W-7405-Eng-48.

† Iowa State University, Ames, Iowa 50011.

0021-9991/81/050167-25$02.00/0

discretizations and boundary conditions, and (4) a discussion of these results and some of those obtained using upwinded formulations.

We should mention that there are other FEM researchers attempting to mimic the "successes" of upwinding demonstrated by finite difference practitioners. Although most of these have been applied to the related advection–diffusion equation (see the ASME Symposium referred to in Ref. [6] for a list of references and numerous discussions on the subject of upwinding), Zienkiewicz and Heinrich [3] have been employing upwind methods on the Navier–Stokes equations. They use different techniques than those of Hughes *et al.*, based on the ideas presented in Heinrich *et al.* [4], and it is not yet clear which of the two "competing" schemes is better. We should also mention that the optimal upwind method employed in [1] has been improved and thus superseded by Hughes *et al.*, in their contribution to Ref. [6]; additionally, they are still striving for schemes which are even better [5].

However, we still believe, and will attempt to demonstrate, that the conventional (Galerkin) treatment of the advection terms, which generates predominantly "centered difference-like" approximations, is usually to be preferred because it has the important property that it can alert the analyst to potential solution difficulties associated with a mesh which is too coarse to resolve certain difficult, but important, features of the flow field such as boundary layers or singularities. The example in this paper is a detailed treatment of one of the examples discussed in Gresho and Lee [6], in which (i) further arguments in favor of conventional Galerkin methods are presented and (ii) it is pointed out that FEM workers are rediscovering some of the lessons regarding upwind schemes and their inadequacies previously learned in finite difference simulations.

Statement of Problem

The basic simulation is that of laminar flow over a square step which forms a portion of the lower boundary of the domain. Following the work of Hughes *et al.*, we located the step fairly close to the inlet region. For most of the simulations, the top boundary is located near the top of the step and is a no-slip wall; i.e., we are considering flow in a channel containing a step. In order to estimate the effects of the confining upper surface, several simulations were also made which are intended to roughly approximate the flow over a step in a partially unbounded flow. Finally, one simulation was made using a symmetry boundary condition at the upper "surface." We should point out that this particular problem, while interesting in its own right, and technically difficult owing to boundary layers and sharp corners, was somewhat secondary to our major goal of demonstrating that affordable high-quality solutions are usually attainable using the conventional FEM. Nevertheless, the results to be presented for this problem may well represent the most accurate numerical simulations reported to date.

We appreciate the goal of some researchers of obtaining accuracy away from thin boundary layers without actually resolving these boundary layers in any detail. While we sympathize with these objectives, we also believe that there are many important situations where such approaches prove difficult, if not impossible; e.g., in the

problem treated in this study, the physics of flow in the region of the upstream corner is, in some sense, as difficult and important as that in the downstream recirculation region and cannot, we believe, be accurately simulated if the associated boundary layer is ignored or artificially thickened.

Brief Review of Previous Work

While there are relatively few studies of flow over a step, two related situations have been studied in more detail: (1) flow through a pipe orifice (for which a wealth of experimental data exists) and (2) flow through a channel containing a sudden expansion (the backward-facing step); the latter case has also been the subject of both analytical and experimental studies at low Reynolds number.

(a) *Flow over a step.* Greenspan [7] and Friedman [8] employed the finite difference method (FDM) using the stream-function/vorticity approach with upwind treatment of advection for Re up to 1000. Hughes *et al.* [1] presented several results using the FEM on a very coarse mesh, first showing the alleged deficiency of the conventional Galerkin method, then the "superiority" of the upwind method. For $Re = 200$, the conventional method produced spurious wiggles in the velocity vectors upstream of the step and a reasonable recirculation eddy downstream. The upwind solution generated no wiggles and a somewhat shorter and less intense downstream eddy. As further "proof" of the power of upwinding, they then presented results for $Re = 10^7$ on the same coarse mesh, which we believe is unfortunate in that it merely reiterates the fact that most upwind schemes become basically insensitive to the "input" value of Re (at large Re, most of the viscosity is artificial—i.e., numerical—and the resulting *effective* Re can be many orders of magnitude less than the input value).

Hughes *et al.* introduced a further difficulty into the problem by employing a flat inlet velocity distribution rather than a "fully developed" (parabolic) profile; hence they are in effect treating the problem of *developing* flow over a step since this boundary condition introduces pressure singularities at the inlet wall regions. This leading edge discontinuity was discussed by Wang and Longwell [9], who treated developing Poiseuille flow in a channel without a step.

(b) *Flow through a pipe orifice.* Since a pipe orifice is commonly used as a flow metering device, it is not surprising that there are more investigations of these flows than of flow over a step. These flows were simulated via FDM by Mills [10], Greenspan [11], Mattingly and Davis [12], and Nigro *et al.* [13].

(c) *Flow through a channel with a sudden expansion.* The numerical simulation of the simpler back step problem has been treated very extensively by Roache and Mueller [14] and analytically by Moffatt [15]—briefly—and in more detail by Weinbaum [16]. Roache and Mueller used the FDM with upwind differencing; detailed results are presented for Re from 0.1 to 100. One of the key results is the numerical demonstration of the fact that the flow separates even for Stokes flow (giving a small corner eddy) and that the separation point moves up the face of the

step, approaching the corner as Re is increased. These effects were previously predicted by Kawaguti [17] and were verified experimentally by Matsui *et al.* [18] for a range of Re from ~5 to ~50. In general, of course, separated Stokes flows have been known for some time; e.g., in lubrication theory [19].

Weinbaum also predicted that separation could occur below the sharp corner and even predicted an approximate form of the corner singularity via analysis of the biharmonic equation for the stream function and the argument that Stokes flow will prevail sufficiently close to the corner.

Finally, Hutton and Smith [20] have recently reported successful simulations of this flow employing, like we, the conventional FEM (no upwinding).

Technical Approach

We believed initially that the cause of the wiggles (other than "central differencing"!) was manifold and designed an experimental program which might separate (and rank) the various contributors and thereby improve our overall understanding regarding numerical "solutions" of the Navier–Stokes equations. The wiggles were believed to be caused by a combination of the following factors:

(1) Too coarse a grid to resolve the steep gradients occurring in the direction of flow.

(2) Inlet boundary conditions and the resulting leading edge singularities.

(3) Proximity of the inlet region to the step (and fixed velocity boundary conditions at the step).

(4) The sharp edge singularity at the leading corner of the step.

In the remainder of the paper, we will briefly discuss the equations and solution method employed, present a summary of our numerical experiments and findings, discuss the implications of these resuts, and draw conclusions relevant to our stated objectives.

Navier–Stokes Equations and Spatial Discretization

The equations of motion and continuity (momentum and mass conservation, respectively) for a constant property, incompressible Newtonian fluid are the Navier–Stokes equations, written here in stress-divergence form:

$$\rho \mathbf{u} \cdot \nabla \mathbf{u} = \nabla \cdot \underline{\tau}, \tag{1a}$$

$$\nabla \cdot \mathbf{u} = 0, \tag{1b}$$

where $\mathbf{u} = (u, v)$ is the velocity vector, ρ is the density,

$$\tau_{ij} = -P\delta_{ij} + \mu \left(\frac{\partial u_i}{\partial x_j} + \frac{\partial u_j}{\partial x_i} \right) \tag{1c}$$

is the symmetric stress tensor, P is the pressure, μ is the viscosity, and δ_{ij} is the Kronecker delta. Given appropriate boundary conditions, Eq. (1) can be used to obtain the velocity components (u and v) and the pressure (P).

The spatial discretization of these equations is performed via the conventional Galerkin finite element method (on the weak form of Eq. (1)) wherein the velocity and pressure are approximated by

$$\mathbf{u} = \sum_{j=1}^{N} \mathbf{u}_j \phi_j(\mathbf{x}) \tag{2a}$$

and

$$P = \sum_{j=1}^{M} P_j \psi_j(\mathbf{x}), \tag{2b}$$

where there are N "free" velocity nodes and M pressure nodes in the discretized domain. The basis functions for velocity approximation, $\phi_i(\mathbf{x})$, are piecewise polynomials which are one degree higher than those for pressure approximation, $\psi_i(\mathbf{x})$, for reasons enumerated previously (e.g., Olson and Tuann [21]; see also Sani *et al.* [22]). Although our element library contains several types of quadrilateral isoparametric elements, in this study we use only one: it has nine nodes and employs biquadratic approximation of the velocity and (using only the four corner nodes) bilinear approximation of the pressure. Upon substituting Eq. (2) into the weak form of Eq. (1) and using $\{\phi_i\}$, $\{\psi_i\}$ as test functions for Eqs. (1a) and (1b), respectively, the following discretized equations are obtained (written in a compact matrix form):

$$[K + N(u)]u + Cp = f, \tag{3a}$$

$$C^{\mathrm{T}}u = g, \tag{3b}$$

where u is the global vector (length $2N$) of the nodal velocities (u_i and v_i), p is a global vector (length M) of the nodal pressures (p_i), f is a $2N$ global vector which incorporates the appropriate boundary conditions in velocities or surface tractions, and g is an M vector incorporating the effects of specified velocities. (Note that no provision is made for employing pressure boundary conditions as they are not allowed—the conservation of mass is violated if pressures are specified along any portion of the boundary; see Gresho *et al.* [23].) K is the $2N \times 2N$ viscous matrix, $N(u)$ is the $2N \times 2N$ nonlinear advection matrix (obtained, as are all others, by "exact" integration using a sufficiently accurate Gauss–Legendre quadrature rule (3×3 generally suffices; see Leone *et al.* [24]), thereby generating an accurate and *consistent* ("conventional") "centered difference" approximation to $\mathbf{u} \cdot \nabla \mathbf{u}$ (as shown in [6] for the simpler four-node element, the conventional FEM generates an advection approximation which is mostly "centered," but which also contains some upwind *and* downwind contributions), C is the $2N \times M$ pressure gradient matrix and its transpose, C^{T}, is the $M \times 2N$ divergence matrix. Details of the formulation and

matrix definitions are omitted as they are space-consuming and have been adequately detailed many times (e.g., Gartling and Becker [25], Gresho *et al.* [23]).

Equation (3), which describes a nonlinear algebraic system in u and P, is solved by the Newton-Raphson method which leads to the following sequence of linear systems (for δu, δp),

$$\begin{pmatrix} K + N(u_m) + N'(u_m) & C \\ C^{\mathrm{T}} & 0 \end{pmatrix} \begin{Bmatrix} u_{m+1} - u_m \\ p_{m+1} - p_m \end{Bmatrix} = \begin{Bmatrix} f \\ g \end{Bmatrix} - \begin{pmatrix} K + N(u_m) & C \\ C^{\mathrm{T}} & 0 \end{pmatrix} \begin{Bmatrix} u_m \\ p_m \end{Bmatrix}, \tag{4}$$

for $m = 0, 1, \ldots$, where $(m + 1)$ is the iteration number. In the Jacobian matrix, the additional matrix, $N'(u_m)$, represents terms such as $\partial u/\partial x$, etc. (whereas $N(u)$ corresponds to the advection operator $\mathbf{u} \cdot \nabla$). We compute our nonlinear (and linear) Jacobian matrix terms analytically, element by element, and store all resulting triply (and doubly) subscripted arrays on disk. The linear systems are solved using a disk-based unsymmetric frontal solver without pivoting, largely based on Hood's [26] published version. Using as an initial guess the solution from a lower Reynolds number (or, as a worst case, from Stokes flow), the solution to Eq. (4), which is defined such that a relative RMS norm on δu is sufficiently small (10^{-5}–10^{-4} in this study), typically requires 5–10 iterations (only one or two iterations are required once the zone of quadratic convergence is reached).

Numerical Experiments

Following Hughes *et al.*, we attempted to simulate the developing flow in a one-unit-high (the characteristic length for defining Re) channel containing a step located 1.2 units from the inlet which is 0.4 units high and 0.4 units across. The inlet boundary condition is a "flat" velocity profile, $u = 1$ and $v = 0$, except that $u = 0$ on the top and bottom no-slip surfaces. No-slip boundary conditions were used everywhere else except at the exit, where traction-free conditions (the natural boundary conditions associated with Eq. (1)) were generally employed (zero normal and tangential stress):

$$f_n = f_x = -P + 2\mu \frac{\partial u}{\partial x} = 0, \tag{5a}$$

$$f_t = f_y = \mu \left(\frac{\partial u}{\partial y} + \frac{\partial v}{\partial x} \right) = 0. \tag{5b}$$

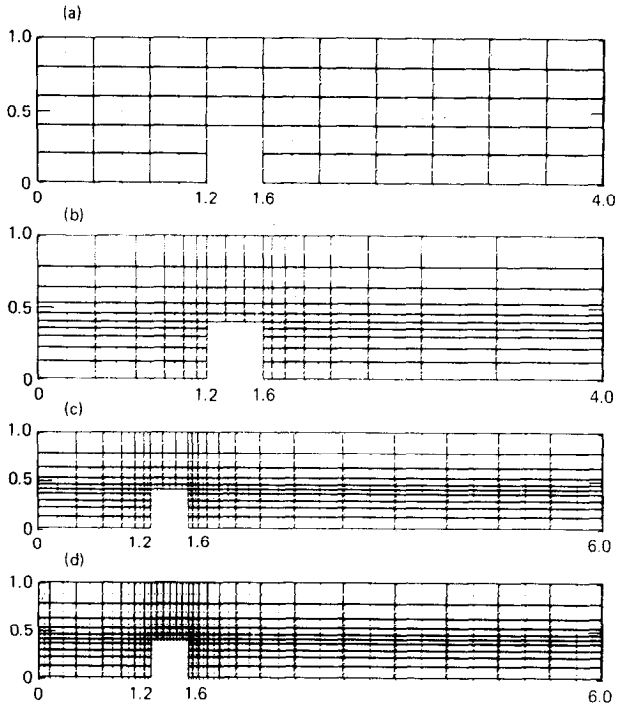

FIG. 1. Grids: a. (Grid 1) Original coarse grid of Hughes *et al.* (48 elements, 227 nodes). b. (Grid 2) First refined grid (155 elements, 685 nodes). c. (Grid 3) Extended version of Grid 2 (205 elements, 895 nodes). d. (Grid 4) Finest grid—more detail at inlet and across step (230 elements, 1003 nodes). Grids 3A and 4A have the top two rows of elements of grids 3 and 4, respectively stretched to extend the domain to $y = 2$.

The overall length of the channel was either 4 or 6 units, as we found a continuing need for a longer channel. The sequence of discretized meshes, ranging from the coarse mesh of 48 elements (a la Hughes *et al.*) to the finest mesh of 230 elements, which reflects the observed requirement for finer meshes as we looked more closely at the solution details, is shown in Fig. 1.

Consistent with the goals stated earlier, and with our hypotheses regarding the causes of the wiggles, we designed a (semi-)systematic sequence of numerical experiments. Since the total number of computer runs became quite large, we must omit a good fraction of them; Table I presents a summary (approximately chronological) of the results we believe to be most relevant. Even this abbreviated list is too long to discuss in much detail; we hope tha the table is largely self-explanatory, but we will discuss certain salient results from this list of experiments in some detail.

Figure 2 shows an appropriate starting point; the Stokes flow ($Re = 0$) solution on the coarse grid. The noteworthy features of this result are the vector wiggles at the inlet and outlet (even Stokes flow can have wiggles). These wiggles are, of course, unrelated to advection and are explained as follows: the inlet wiggles are caused by

TABLE I

Summary of Relevant Numerical Experiments

Run No.	Grid	Reason for run	Key input	Results/comments
1	1	Stokes flow	$Re = 0$	Inlet wiggles due to singularity, outlet wiggles due to zero traction. (See Fig. 2.)
2	1	Duplicate Hughes *et al.* [1] results	$Re = 200$	Wiggles upstream of step; eddy downstream. (See Fig. 5a.)
3	1	Seeking effective Re of Hughes *et al.*	$Re = 100$	Smaller wiggles, smoother eddy.
4	1	Ditto	$Re = 50$	Smaller wiggles, smoother eddy. Based on coarse grid and eddy size, $50 < Re < 100$ for upwinded.
5	1	Relax inflow B.C.	$Re = 0$; $f_n = P(y)$ from Run 1	Essentially the same as Run 1.
6	1	Ditto at $Re = 200$	$Re = 200$; $f_n = P(y)$ from Run 2	No solution (diverged); indicates "problems" with this grid and $Re = 200$. (This technique also failed for $Re = 100$; succeeded for $Re = 25$.) (See also Runs 21 and 22.)
7	Channel flow. (no step)	Brief study of inlet pressure singularity	$Re = 0$	Inlet and outlet wiggles, top and bottom; decay quickly. High pressure at inlet corners; suggests, for Stokes flow, that inlet wiggles are caused by the corner singularity.
8	Ditto	Ditto at $Re = 200$	$Re = 200$	Wiggles much smaller, but last longer; still get high pressure at inlet corners.
9	Ditto	Eliminate singularity	$Re = 0$; $f_n =$ constant at inlet	No inlet wiggles, no singularity; exact (Poiseuille) solution except at outflow. This (or parabolic $u(y)$) is probably a better boundary condition (B.C.).
10	1	Try to eliminate wiggles for Stokes flow with step	$Re = 0$; $u(y) =$ parabola	Inlet wiggles eliminated. (See Fig. 3.)
11	1	Ditto for $Re = 200$	$Re = 200$; $u(y) =$ parabola	Small effect (10–15%); wiggles and inlet corner pressure slightly reduced. Thus, retain original inflow B.C. (See Fig. 5c.)

12	1	Assess effect of proximity of step to inlet region	$Re = 200$, a la Run 2, but reversed flow direction	Wiggles are just as large near step and extend (damped) back to inlet. Somewhat surprisingly this was not (even partially) a cause of the wiggles. (See Fig. 5b.)
13	2	Need finer grid	$Re = 0$	Small symmetric upstream and downstream eddies; still some inlet and outlet wiggles, but small; also, pressure and (small) vertical velocity wiggles across top of step. (See Fig. 4.)
14	2	Improve inlet $u(y)$; see text;	$Re = 0$; smoother inlet B.C. (no overshoot)	Small improvement in corner pressure and size of wiggles. Retain this B.C. to simulate $u = 1$ at inlet.
15	2	Test finer grid at $Re = 200$	$Re = 200$ (smoother inlet B.C.)	Wiggles upstream of step are gone; extremely small inlet wiggles from inlet pressure singularity. Now the eddy is too long for the grid. (See Figs. 6, 7a.)
16	2	Ditto, but eliminate inlet singularity	$Re = 200$; $u(y) =$ parabola	Better inlet flow pattern; no wiggles at all. Most of solution looks very much like Run 15, however.
17	3	Original domain too short to contain eddy	$Re = 200$ a la Run 15	Eddy details are now acceptable. Here, however, traction free outflow B.C. causes minor wiggles (flow wants to be unidirectional, but outflow B.C. precludes it). (See Figs. 7b, 8.)
18	3	Seeking effective upwinded Re (Hughes *et al.*) on fine grid	Ditto except $Re = 85$	Based on eddy length, this looks like the effective Re for upwinded scheme on Grid 1 (vis-a-vis $Re = 200$). (See Fig. 9.)
19	4	Seeking better solution near singularities	$Re = 0$, a la Run 13	Inlet wiggles essentially eliminated; finer zoning at inlet is useful, especially for Stokes flow (see also comments on next run).
20	4	Seeking better solutions near singularities	$Re = 0$, a la Run 14	Overall solution little different from Grids 2, 3, or 4; wiggles generally reduced on grid 4, but pressure singularities at corners of step are still large (and vertical velocity still oscillates above top of step).
21	4	Ditto at $Re = 200$	$Re = 200$, a la Runs 15, 17	Little different from Run 17, except in smallest details near top of step; Grid 3 was adequate for most purposes.

TABLE I—*Continued*

Run No.	Grid	Reason for run	Key input	Results/comments
22	4	Relax inflow B.C. (cf. Run 6)	$Re = 200$; $f_n = P(y)$ from Run 21	Converged nicely; results close to those in Run 21, except for details near inlet.
23	3A	Attempt to analyze semi-infinite domain ($f_n = f_t = 0$ at top)	$Re = 200$; extend vertical dimension from 1 to 2; outlet B.C.'s: $u = u$ (inlet), $v = 0$	Did not converge; outflow B.C.'s incompatible with internal flow field.
24	3A	Ditto except relax outflow B.C.'s	$Re = 200$; outlet B.C.: $f_n = 0$, $v = 0$	Very long eddy, which leaves grid; downstream wiggles, (from outlet, almost back to the step). B.C.'s still incompatible—vertical velocity should not be zero. (See Fig. 10.)
25	3A	Ditto except further relax outflow B.C.'s	$Re = 200$; $f_n = f_t = 0$ at outlet	Better—no wiggles. Very large eddy which separates from top of step and "leaves" the grid: need still longer domain to get full details of eddy (not done). (See Figs. 11, 12.)
26	4A	Ditto Run 25 with finest grid	Same as Run 25	Very close to Run 25, except details (e.g., separation point) near top of step. Need finer grid yet if all details near step are required (not done). (See Fig. 13.)
27	3	Comparison with Roache and Mueller [14]	Like Run 17 except top B.C. changed to $f_t = v = 0$	Very significant effect; eddy is much longer (it leaves the grid) and stronger.

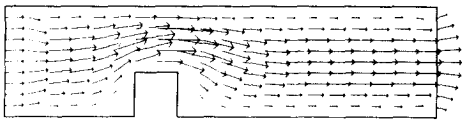

FIG. 2. Stokes flow solution for "flat" inflow profile on Grid 1.

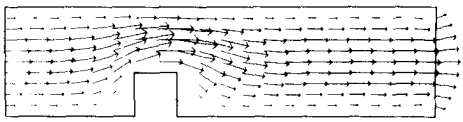

FIG. 3. Stokes flow solution for parabolic inflow profile on Grid 1.

the leading edge singularities (high pressures are generated at the corners where the fluid decelerates and converges toward mid-channel) and the outlet wiggles, and general flow divergence there, are caused by an inherent incompatibility in boundary conditions. It is clear that the flow is striving toward the unindirectional distribution associated with Poiseuille flow, for which case $u = u(y)$, $v = 0$, and (especially) $\partial v/\partial x = 0$. But the outlet boundary condition of zero shear stress (Eq. (5b)) requires $\partial u/\partial y + \partial v/\partial x = 0$; noting that u must be zero at the top and bottom walls implies that $\partial u/\partial y \neq 0$. Hence $\partial v/\partial x \neq 0$ and a (shear) stress-free boundary condition is *not* compatible with a parallel flow. Although for this simple case, it is easy to remedy this "problem" (either $v = 0$ or a linear distribution of imposed shear stress would do it), it turns out that the stress-free natural boundary condition is one of the best outflow boundary conditions under many conditions of more complex flows at higher Re (where the outlet conditions are truly unknown and where inertial effects become important relative to viscous effects). For further discussion of the outflow boundary condition, see Hutton and Smith [20] and Gresho *et al.* [23].

The inlet wiggles are also easy to eliminate; Fig. 3 shows the effect of a parabolic (fully developed) inflow boundary condition—there are no inlet singularities and no inlet wiggles. See also Runs 7–9 in Table I, which prove these points on a simple (no step) channel flow using a 10×5 grid.

Figure 4a shows a finer grid (Fig. 1b) version of the Stokes solution of Fig. 2; while the inlet and outlet wiggles are still present (the grid is still coarse in these regions), they only slightly affect the interior details of flow near the step. The streamlines for this case are shown in Fig. 4b, where the symmetric upstream and downstream corner eddies are now resolved by the finer grid. It is noteworthy that the restrictive domain and boundary conditions at the channel top causes much smaller eddies than would occur in a more unbounded flow. Thus, the results of Roache and Mueller [14], the beautiful experimental results of Taneda [27], and some of our own results using different domains and boundary conditions at the top, all display larger eddies (the separation point is much closer to the top of the step). All streamline plots

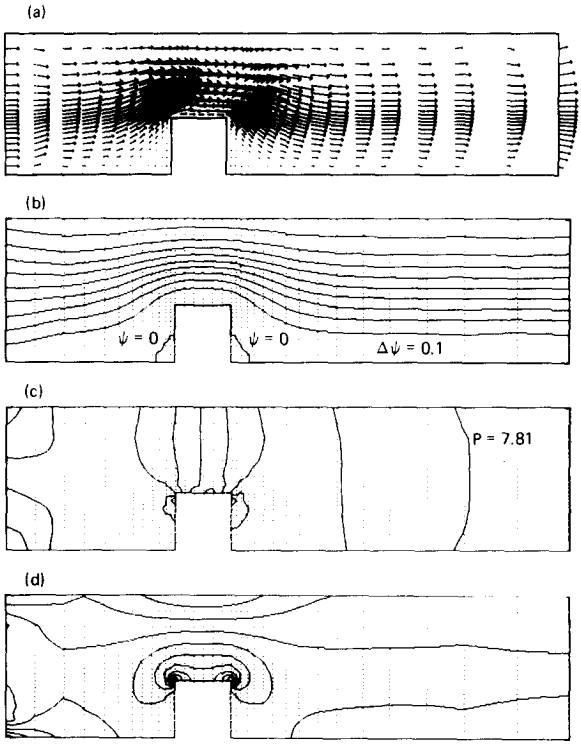

FIG. 4. Stokes flow solution for "flat" inflow profile on Grid 2. a. Vector field. b. Streamlines. c. Isobars ($\Delta P = 10.1$). d. Vorticity contours.

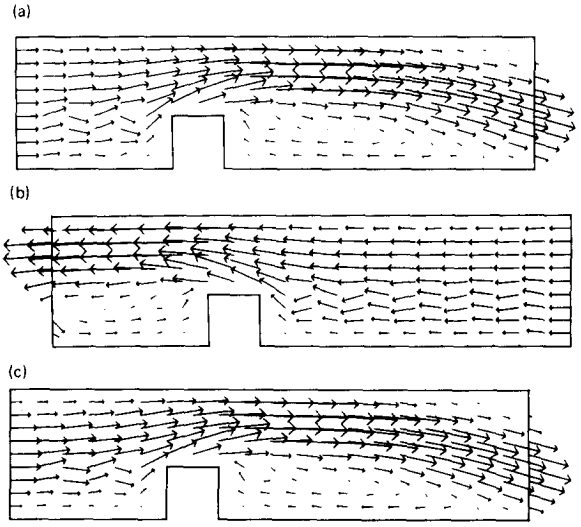

FIG. 5. Solutions for $Re = 200$ on grid 1. a. "Flat" inflow profile. b. "Flat" inflow profile with flow direction reversed. c. Parabolic inflow profile.

were prepared using a minimally adjusted velocity field (as described in Sani *et al.* [28]) and contour integration over element boundaries. The "adjusted" velocity is required in order to assure element mass balances and good streamlines; it generally has an imperceptible visual effect on the velocity vector plots. The corresponding pressure field, Fig. 4c, clearly shows the effect of the leading edge singularities and the significant variation of pressure near the step (the pressure in this figure is made dimensionless by $\mu u_0/l$). Finally, the vorticity contours are presented in Fig. 4d, showing the effect of vorticity generation at the sharp corners and the overall symmetry (near the step) associated with Stokes flow. Vorticity contours were computed using "Scheme 4" of Lee *et al.* [29] in which the 3×3 Gauss point values of computed vorticity from $\omega = \partial v/\partial x - \partial u/\partial y$, are linearly extrapolated back to the nodes after which simple averaging is employed (our contour ploting package requires nodal values; otherwise we would contour the Gauss point values directly—and probably those from the more accurate 2×2 Gauss points).

We now move on to the nonlinear problem with $Re = 200$, beginning with the coarse mesh of Fig. 1a. In Fig. 5a is our version of the wiggly solution criticized by Hughes *et al.* [1], who made the statement which triggered this study: "We believe this problem demonstrates the inappropriateness of Gauss–Legendre integration of the convection term." The inlet wiggles now appear to be caused more by the presence of the step than the leading edge singularity since they are strongest near the step. The outlet wiggles are now absent, owing to the importance of the inertia terms at this *Re*.

To determine the importance of the close proximity of the step as a cause of the wiggles, we reversed the flow direction to obtain the result shown in Fig. 5b. It thus appears that the step location has nothing to do with the cause of the wiggles; presumably they occur independently of the location of the inlet, are of maximum amplitude near the step, and are only slowly damped in the upwind direction.

In Fig. 5c are shown the results of removing (or reducing) the leading edge singularity by using the parabolic velocity profile as an inlet boundary condition. The wiggles are only slightly reduced (10% or so), and another potential cause of the wiggles is largely eliminated.

Having narrowed the main causes to the steep gradients in the flow direction associated with the presence of the step, the associated pressure singularities, and the inability of the coarse grid to deal with them, we generated our first (graded) fine mesh (Fig. 1b) and repeated the computations (for which the Stokes flow results have already been discussed). Before presenting these results, however, we disgress briefly to introduce our better (smoother) inlet boundary condition when a "flat" profile is desired, since it is employed in all subsequent computations. When piecewise quadratic approximation is used for the velocity, the inlet velocity profile resulting from employing $u = 0$ at the walls and $u = 1$ at all nodes in between, displays an awkward maximum ($u_{\max} = 1.125$) in the element containing the wall boundary (and

(inflow) midside nodes of these walls elements, thus causing $u(y)$ to increase

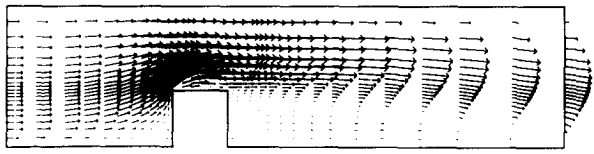

FIG. 6. Solution for "flat" inflow profile, $Re = 200$, on grid 2.

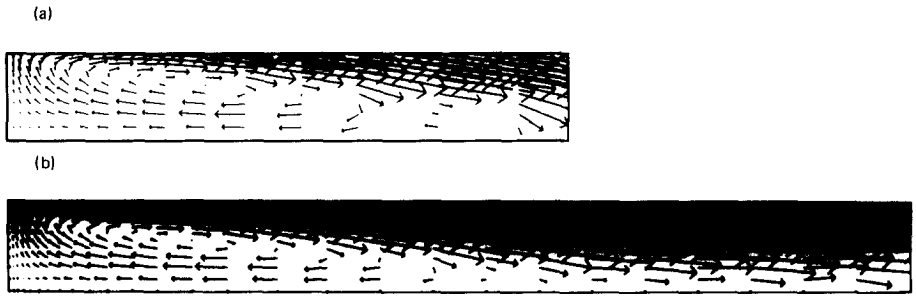

FIG. 7. Details of downstream eddy region for $Re = 200$: a. Grid 2, showing spurious double eddy. b. Grid 3, showing single eddy.

smoothly to 1.0 at the second node from the boundary (and it has zero slope there). This is the "smoother inlet B.C." referred to at Run 14 in Table I.

Figure 6 shows the finer grid solution for $Re = 200$ and demonstrates that the wiggles were caused by the poor resolution of a rapidly changing flow field near the step (since they are now absent). Now that we have a better solution, however, the eddy length has increased and caused a "new (minor) problem"—the eddy is too long for the grid and the flow field experiences some perturbations via interaction with the outflow boundary conditions. The result is a sort of spurious second eddy near the outlet, as shown in Fig. 7a (which is a blowup from Fig. 6). This led to our third grid (Fig. 1c), which is basically an extended version (to $x = 6$ rather than 4) of grid 2. Repeating the calculation for $Re = 200$ showed, as expected, the appropriate change in the eddy details near $x = 4$, which is shown in Fig. 7b (there is no spurious second eddy). It also showed, unfortunately, a reintroduction of small outflow wiggles caused, presumably, by the same incompatibility referred to earlier; this problem appears to be most prominent when the outflow "wants to be" unidirectional close to a no-slip wall. The streamlines, pressures, and vorticities on this sufficiently long grid are shown in Fig. 8. Figure 8a shows a very small upstream eddy and a downstream eddy of length ~ 2.7 (6.75 step heights). The isobars of Fig. 8b *clearly* show the need for fine zoning near the leading corner singularity and provide further evidence of the cause of the original wiggles (i.e., they are the result of gradients which are too steep to be captured by a coarse mesh). The vorticity distribution, Fig. 8c, shows large generation at or near the corners as well as at the inlet lower boundary, and its advection downstream.

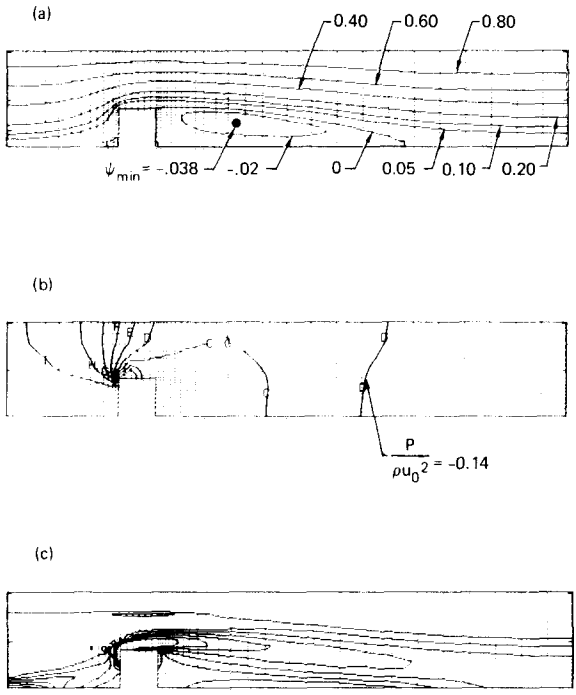

FIG. 8. Additional results for $Re = 200$ on grid 3: a. Streamlines. b. Isobars ($\Delta P/\rho u_0^2 = 0.240$). c. Vorticity contours.

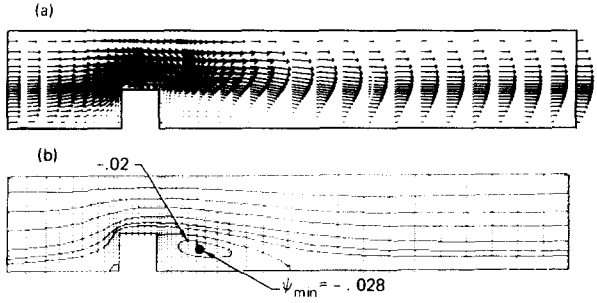

FIG. 9. Solution for $Re = 85$ on grid 3: a. Vector field. b. Streamlines.

Having resonably adequately resolved the flow at $Re = 200$, we used the same grid to estimate the *effective* Re in the upwinded simulation of Hughes *et al.* Figure 9 shows the results for $Re = 85$; based on eddy length (the only convenient measure), this represents our best estimate of their effective Re (note also the near absence of an upstream eddy at this Re and that separation occurs just below the corner). Examination of Figs. 4b, 8a, and 9b reveals that the upstream eddy is smallest at

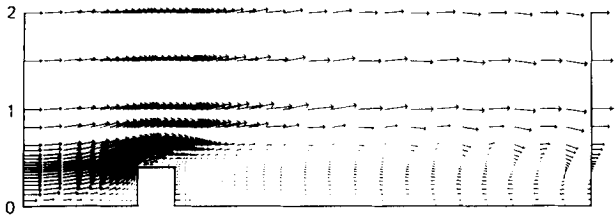

FIG. 10. Unconfined channel simulation for $Re = 200$, showing outflow boundary condition problems (grid 3a).

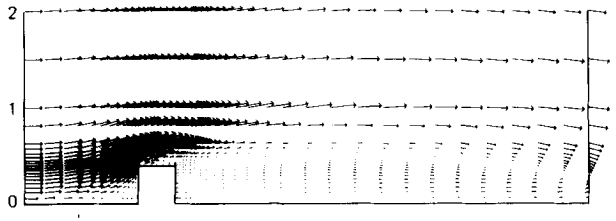

FIG. 11. Same as Fig. 10 except better outflow boundary conditions.

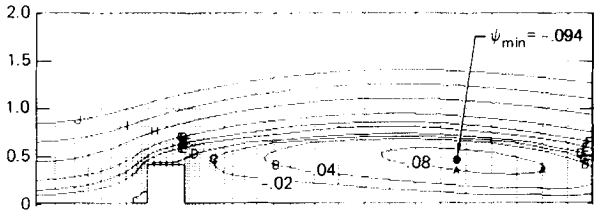

FIG. 12. Streamlines for unconfined channel simulation at $Re = 200$ on grid 3a (corresponding to Fig. 11).

$Re = 85$ while the downstream eddy size increases monotonically with Re. These results are in general agreement with those of Friedman [8] and Mills [10].

Since all of these channel flow simulations indicated that separation occurred at (or slightly below) the trailing corner of the step (for $65 < Re < 200$), we performed a few experiments intended to approximate flow over a step in an unbounded fluid to determine the effects of the confining upper wall and to see whether separation would occur closer to the leading corner. Since this was more or less an afterthought, we performed only limited analysis: (1) we did not increase the number of elements in the vertical (rather, we stretched the vertical extent from 1.0 to 2.0—the Reynolds number is still based on $l = 1$—by grading the mesh), (2) we did not lengthen the grid beyond 6 units. In order to model the semi-infinite domain in the least restrictive manner, we imposed traction-free boundary conditions at the top boundary to permit outflow and inflow. Figure 10 shows the results for $Re = 200$, on extended grid 3 (grid 3A), using an outflow boundary condition of zero vertical velocity (we

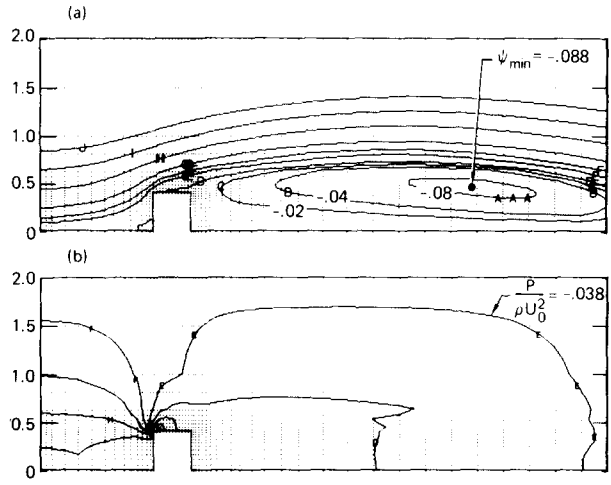

FIG. 13. Unconfined channel simulation for $Re = 200$ on the finest grid (4a): a. Streamlines. b. Isobars ($\Delta P/\rho u_0^2 = 0.138$).

erroneously expected a nearly parallel flow) and zero normal stress. Here we see *another* cause of very noticeable wiggles; the outflow boundary condition is too restrictive relative to what the flow "wants to be." (Would upwinding "cure" these, too? We believe that it would.) Once again, the conventional Galerkin FEM has alerted us to a simulation deficiency. Thus, we modified the outflow boundary condition from $v = 0$ to $f_t = 0$ and the much-improved results are shown in Fig. 11; there are no wiggles and this outflow boundary condition again causes minimal interference with the interior flow. The corresponding streamlines are displayed in Fig. 12 and show: (1) the flow now separates from the top of the step (downstream of the leading corner) and (2) the eddy is stronger, higher, and longer than that for channel flow (it is, of course, too long for this grid to fully resolve). Finally, Fig. 13 shows some results from the same simulation performed on our (vertically extended) finest grid (grid 4A, Fig. 1d), in which we improved the mesh at the inlet and across the top of the step (there were other reasons for generating this fourth grid, which are outlined in Table I and further discussed later). Comparing Figs. 12 and 13a it is seen that the finer grid has caused a shift in the separation point and a slight (~6%) decrease in the eddy strength. Additional fine zoning very close to the step, and a longer (and probably higher) domain would be required to provide a truly accurate result for this case. The isobars corresponding to this run are shown in Fig. 13b, and may be compared with those in Fig. 8b.

In our final simulation (Run 27 of Table I), we modified our top boundary condition from a no-slip wall to a stress-free symmetry condition (like those used for pipe orifice calculations) in order to approximately simulate the results of Roache and Mueller [14], who showed what we believed at first to be an exceptionally long eddy for $Re = 100$ (they used step height to define Re; on this basis, our results at

TABLE II

Summary of Computer Cost

Run number	Number of elements	Number of equations	CPU time (sec/iteration)	Number of iterations to $Re = 200$ (starting from Stokes solution)
2	48	520	2.4	9
15	155	1558	10.8	6
17	205	2033	14.8	5
21	230	2278	16.6	5

$Re = 200$ correspond to theirs at $Re = 80$)—and with *upwinding* yet—their eddy length was 7.5 step heights (vs ~6.75 for our channel flow). The results were interesting and reassuring: at $Re = 200$ ($Re = 80$ a la Roache and Mueller), our eddy length was approximately 15 step heights (this is quite approximate, since our grid ended at 11 step heights and we extrapolated the separation streamline); the minimum value of the stream function in the vortex was ~ -0.043. Separation occurred at the trailing corner and the separation streamline pointed slightly upward (similar to, but much less than, that shown in Figs. 12 and 13a), in apparent agreement with some of the analytical results of Weinbaum [16]. The most important additional result from this and the previous simulations is that the location of the separation point and the

relative to less confined configurations.

Although our current code is a "research" code in that it contains many unused options and is not very "streamlined," some cost data may still be of interest. Table II shows the total CPU cost (including I/O, which is typically 20–40%) on a CDC-7600 for the four grids employed in this study. For the last three grids, the cost varies approximately with the 1.13 power of the number of equations, which may not be too surprising since the "front width" is constant for these three grids.

Discussion

Additional insight into the nature of the difficulties inherent in this simulation is revealed in the pressure profiles shown in Figs. 14–16. In Figure 14 are shown the surface pressure distributions on and near the step for Stokes flow from three different grids. The existence of (symmetric) pressure singularities is clearly revealed; even the finest grid has not adequately resolved the singularities, as evinced by the oscillations across the top of the step. It appears that the singularities are located near the corners, but on the vertical sides of the step; the similarity in the extrema from grids 2 and 4 might also suggest that the pressure is finite at these discontinuities. These observations are not in accord with the results of Weinbaum [16],

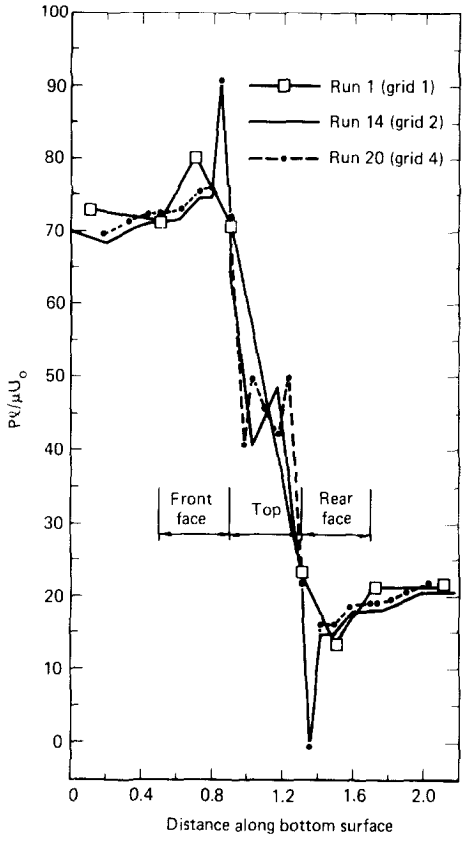

. 14. Surface pressure distribution near and on the step for Stokes flow.

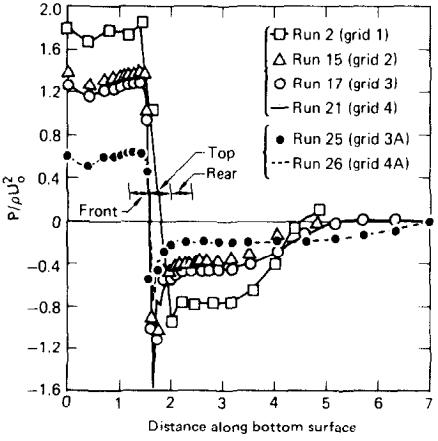

FIG. 15. Pressure distribution on lower boundary for $Re = 200$.

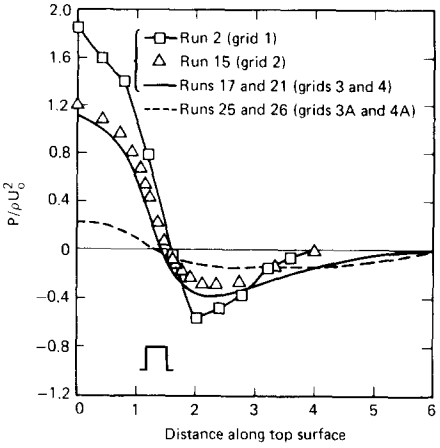

FIG. 16. Pressure distribution at $y = 1.0$ for $Re = 200$.

who predicted infinite pressures at the corners ($P \sim \pm 1/r^{0.456}$); our grid is apparently too coarse the reveal the true behavior very close to the corners. The pressure oscillations appear to be localized, however, since the pressures are quite smooth at the first "row" of interior nodes. Also, the vertical component of velocity changes sign several times along the first row of nodes above the top of the step, further indicating that our solution, even on the finest grid, is not yet correct in all details (there are still some very small wiggles). The corresponding pressures for $Re = 200$ are presented in Fig. 15 and seem to indicate that the pressure singularity is somewhat less severe for this case, although the gradient near the leading corner is very large. The differences in the solution between grids 3 and 4 are quite small in general, although the pressure minimum along the top of the step is not so well resolved by grid 3. Again, these results differ from those of Weinbaum in that the presence of the inertial terms has significantly affected the surface pressure field. Finally, the much smoother pressure distribution along $y = 1$ (which is the top wall for the channel flows) is presented in Fig. 16.

We believe that a partial explanation of the smoother pressures from the Navier–Stokes equations than from the Stokes equations is the following: In Stokes flow, the pressure satisfies the Laplace equation and the only source of singularities can be on the boundary (and these effects are rapidly damped away from the boundaries owing to the well-known smoothing property of the Laplacian); hence, the pressure can vary much more rapidly on the boundary than in the interior. In Navier–Stokes flow, however, the pressure satisfies a Poisson equation whose "source term" (composed of products of first derivatives of u and v), if "well behaved" and sufficiently "strong," can mitigate the effects of boundary-caused singularities; hence, the solution can be smoother, even on the boundary. In a discretized solution to the Navier–Stokes equations, the source term may not be so "well behaved" on a coarse mesh, and the mitigating effects may then be absent; in

fact, the reverse can occur. In this case, the hyperbolic nature of the advection terms will propagate the "problem" to other parts of the domain in the form of wiggles or oscillations; i.e., spurious "noise" is "generated" by the too-sharp gradients and "radiated" by the advection terms when the mesh is too coarse. These effects are absent in most upwinded simulations because of numerical diffusion.

As a result of our numerical experiments (including one not yet discussed in which we "rounded" the sharp corners by moving several of the nodes defining the step—the results, on the coarse grid, showed upstream wiggles which are little different from those for the step) and supporting analysis, we believe we can now more confidently state the principal cause of the wiggles on a coarse mesh: the horizontal component of velocity must go from $O(1)$ to zero in a distance approximately $O(1/Re)$ to $O(1/\sqrt{Re})$ as the flow approaches the step. This requirement forces large gradients in the direction of flow which obviously cannot be "captured" by a coarse mesh. The conventional FEM, with essentially negligible artificial diffusion (which reduces Re and spuriously thickens the boundary layer toward the limit of the mesh interval) responds (and "overreacts") to this situation and generates "noise" (oscillations) which is propagated upstream by the (nonlinear) advection terms. It is, in fact, the (essentially—see Lee *et al.* [30]) nondiffusive central difference nature of these terms, and not the nonlinearity, which is the major *cause* of the error propagation (nonlinear interactions will affect the *results*). For example, even the linear advection–diffusion equation (1-D or 2-D) will generate upstream oscillations under certain conditions (e.g., under the tight constraint caused by specifying the value of the dependent variable at the outflow coupled with a large grid Peclet number. This type of example is also discussed by Hedstrom and Osterheld [2], Gresho and Lee [6], and by Hughes *et al.* in their Figs. 16–18; see also the valid criticism of this computation by Gartling [31], however).

We believe that the proper cure for these wiggles (and those from advection–diffusion when the "specified value" outflow boundary conditions *must* be employed) is to utilize the inherent capability of isoparametric finite elements and rezone in the region causing the wiggles so that the (important) "difficulty" (singularity, boundary layer, etc.) is adequately resolved by the mesh; the bonus accruing from the cost of rezoning (and judicious rezoning need not be too expensive) is that the solution can usually be relied upon once the wiggles have been (properly) reduced or eliminated (see also Gresho and Lee [6]).

Consistent with the above explanation, we believe that the *conventional* Galerkin FEM should especially be employed on all *new* problems; if there are inherent difficulties with the grid selected, (and/or boundary conditions and/or parameter values), the resulting oscillations will identify the locations of these difficulties and provide the impetus to rezone in these regions and thereby obtain a good and valid solution. Upwind methods, on the other hand, may deprive the analyst from obtaining a good solution simply because they are too insensitive to inherent problem difficulties.

The basic fallacy of upwinding (besides "smooth implies accurate"), as pointed out nicely by De Vahl Davis and Mallison [32], is that the *effective* Re is variable

throughout the mesh and is always less than the desired (input) Re; the effective Re approaches the desired Re only in the limit of $\Delta x \to 0$. This can be most easily demonstrated via the one-dimensional advection–diffusion equation, where the Peclet number (Pe) plays the role of the Reynolds number (ratio of advective to diffusive transport):

$$\frac{\partial T}{\partial t} + u\frac{\partial T}{\partial x} = K\frac{\partial^2 T}{\partial x^2}, \tag{6}$$

where u is a prescribed velocity and K is the diffusivity. If upwind finite differencing is employed on the advection term, the numerical result is identical to that in which central differencing is employed on the equation

$$\frac{\partial T}{\partial t} + u\frac{\partial T}{\partial x} = \left(K + \frac{1}{2}u\,\Delta x\right)\frac{\partial^2 T}{\partial x^2}, \tag{7}$$

where Δx is the grid spacing and $\frac{1}{2}u\,\Delta x$ is the artificial (numerical) diffusivity. Nondimensionalizing this equation with l (characteristic length of the problem) for length and l/u for time gives

$$\frac{\partial T}{\partial t} + \frac{\partial T}{\partial x} = \left(\frac{1}{Pe} + \frac{1}{2}\frac{\Delta x}{l}\right)\frac{\partial T^2}{\partial x^2}, \tag{8}$$

where $Pe = ul/K$ is the desired Peclet number. By equating the coefficient of $\partial^2 T/\partial x^2$ to $1/Pe_{\text{eff}}$, the effective Peclet number is obtained as

$$Pe_{\text{eff}} = \frac{Pe}{1 + \frac{1}{2}(\Delta x/l)\,Pe}, \tag{9}$$

from which it follows, for a fixed $\Delta x/l$, that $Pe_{\text{eff}} \approx Pe$ when Pe is small, but $Pe_{\text{eff}} \to 2l/\Delta x$ as $Pe \to \infty$, i.e., there is an upper limit (usually not very large) to the effective Peclet number using upwind techniques. This also explains the relative insensitivity of the results to Re for large Re, as seen, for example, in the work of Greenspan [7]. A similar result for the two-dimensional Navier–Stokes equations is presented by De Vahl Davis and Mallison; for a lid-driven cavity simulation at a desired Re of 1000 on a 31×31 mesh, they show that the effective Re is as low as 240 and that the average effective Re is closer to 400. They also argue that a 100×100 mesh would be required in order for an upwind scheme to obtain a minimum effective Re of 900.

Of course the FEM "optimal upwinding" scheme of Hughes *et al.* may be a significant improvement over the conventional "full upwinding" discussed above (the $\frac{1}{2}$ factor in Eq. (8) can vary throughout the mesh). The optimal upwinding has the nice property that it approaches "central differencing" (i.e., conventional FEM) as the local (element-based) $Re \to 0$; but in the other limit (large local Re), it too approaches "full upwinding" and the effective Re is substantially lower than the

for Pe or Re of $O(10^7)$ on coarse meshes more closely resemble flows with effective Pe or Re of probably more like $O(10^2)$).

Another recent study by Moult *et al.* [33] points out both the good and bad features of upwinding. The good feature of upwind methods (which they utilize) is that they are "robust" in the sense that solutions are easier to obtain than with central differences (especially with iterative solution methods). The bad feature is, of course, that the solutions are often deceptively inaccurate. They therefore combined the features of both methods via FEM and FDM in a stream function/vorticity formulation, using an iteration scheme which "looks like" upwind, but finally yields a solution corresponding to central differences (they effectively solve "many" (several, presumably; they neglected to give details) "upwind sub-problems" in order to converge to a centered difference result).

As a final admonition regarding upwinding, we believe that it is inherently risky because it generates a false sense of security which runs counter to both logic and physics. The false sense of security can result from obtaining *smooth* (and "easy to obtain") solutions with "any mesh" for "any *Re*." The illogical aspect is that the combination of a lower order, less accurate method and a large *Re should* dictate the use of a finer mesh; but upwind schemes are consistently applied on coarser meshes and at higher *Re*. Finally, the physics of fluid behavior is well known to often be a strong function of *Re* in that the flow invariably becomes more complex as *Re* increases (at least for laminar flow); the danger of upwinding (on a coarse mesh) is that the simulation will often not "recognize" these complexities since it, in effect, reduces the effective *Re* by "just enough" to obtain a smooth, "reasonable-looking" solution, which is often (essentially) independent of *Re*. This effect could be particularly deleterious in situations displaying multiple, overlapping boundary layers.

During the final revision of this paper, it was pointed out by a reviewer that there are some new developments for one-dimensional problems which give some hope that one day one may have reliable methods that are more accurate than conventional Galerkin FEM. In particular, the papers by Carroll and Miller and Morton and Barrett from the recent BAIL Conference [34] may ultimately be viable for Navier–Stokes simulations.

Summary and Conclusions

We have identified the major and minor causes of the wiggles in central difference (i.e., conventional FEM) approximations of the Navier–Stokes equations for a particular problem and generalized the results. We have also shown that solutions which are smooth a priori and which do not resolve the boundary layer are not very accurate (at least for this type of problem); grid refinement is required in the critical region near the leading corner.

The numerical results presented, while limited in scope, are believed to be the most accurate available for flow over a step at $Re = 200$. They are probably close to

"converged" (i.e., represent a solution of the Navier–Stokes equations) for the channel case. They are not so well converged for the semi-infinite domain case, which displays a significantly different solution; here the results are merely suggestive. We have also shown that the details of the separated flow behind the step are strongly affected by the upper "boundary condition."

We hope that we have succeeded in demonstrating that the conventional Galerkin FEM is not "inappropriate" for difficult computations. On the contrary, we have attempted to demonstrate that it may be *most* appropriate if one is seeking accurate solutions and have tried to provide sufficient reasons for interpreting many upwind simulations, and the results therefrom, cautiously and even suspiciously.

ACKNOWLEDGMENTS

The authors have benefited from useful discussions with Dr. R. L. Lee of LLL, Professor R. L. Sani of the University of Colorado, and Dr. D. K. Gartling of Sandia Laboratories; their critical reviews of the first draft of this paper are also gratefully acknowledged as is that of Dr. R. C. Y. Chin of LLL.

REFERENCES

1. T. HUGHES, W. LIU, AND A. BROOKS, *J. Comput. Phys.* **30** (1979), 1.
2. G. W. HEDSTROM AND A. OSTERHELD, *J. Comput. Phys.* **37** (1980), 399–421.
3. O. C. ZIENKIEWICZ AND J. HEINRICH, *Comp. Meth. Appl. Mech. Engr.* **17/18** (1979), 673–698.
4. J. HEINRICH, P. HUYAKORN, O. ZIENKIEWICZ, AND A. MITCHELL, *Int. J. Numer. Meth. Engr.* **11** (1977), 131–143.
5. A. BROOKS AND T. J. HUGHES, *in* "Proceedings, Third International Conference on Finite Element Methods in Flow Problems, Banff, Alberta, Canada, June 10–13, 1980."
6. P. GRESHO AND R. L. LEE, *in* "Proceedings, ASME Symposium on Finite Element Methods for Convention-Dominated Flows, Winter Annual ASME Meeting, N.Y., Dec. 1979"; a revised and extended version of this paper will also appear in *Computers and Fluids.*
7. D. GREENSPAN, *J. Engrg. Math.* **3** (1969), 21.
8. M. FRIEDMAN, *J. Engrg. Math.* **6** (1977), 285.
9. Y. WANG AND P. LONGWELL, *A.I.Ch.E. J.* **10** (1964), 323.
10. R. MILLS, *J. Mech. Engr. Sci.* **10 (1968), 133.**
11. D. GREENSPAN, *Int. J. Numer. Meth. Engr.* **6** (1973), 489–496.
12. G. MATTINGLY AND R. DAVIS, *in* "Proceedings, ASME Winter Annual Mtg." paper No. No. 77-WA/FE-13, 1977.
13. F. NIGRO, A. STRONG, AND S. ALPAY, *ASME J. Fluid Engr.* **100** (1978), 467.
14. P. ROACHE AND T. MUELLER, *AIAA J.* **8**, No. 3 (1970), 530.
15. H. MOFFATT, *J. Fluid Mech.* **18** (1964), 1.
16. S. WEINBAUM, *J. Fluid Mech.* **33**, part 1 (1968), 38–63.
17. M. KAWAGUTI, "Numerical Solutions of the Navier–Stokes Equations for Flow in a Channel with a Step," Tech. Summary Rept. 574, Mathematics Research Center, University of Wisconsin, Madison, 1965.
18. T. MATSUI, M. HIRAMATSU, AND M. HANAKI, **in** "Proceedings, Fourth Biennial Symp. on Turb. in Liq., University of Missouri, Rolla, 1975, pp. 29–1, 29–6.
19. H. SCHLICHTING, "Boundary Layer Theory," McGraw–Hill, New York, 1960.

20. A. HUTTON AND R. SMITH, "The Prediction of Laminar Flow over a Downstream-Facing Step by the Finite Element Method," RD/B/N3660, Central Electricity Generating Board, London, England, April, 1979.
21. M. OLSON AND S. TUANN, *in* "Finite Elements in Fluids," Vol. 3, pp. 73–89, Wiley, New York, 1978.
22. R. SANI, P. GRESHO, AND R. LEE, *in* "Proceedings, Third International Conference on Finite Element Methods in Flow Problems, Banff, Alberta, Canada, June 10–13, 1980."
23. P. GRESHO, R. LEE, AND R. SANI, *in* "Recent Advances in Numeical Methods in Fluids," Pineridge Press Ltd., Swansea, U.K., 1980.
24. J. LEONE, P. GRESHO, S. CHAN, AND R. LEE, *Int. J. Numer. Engr.* **14** (1979), 769–773.
25. D. GARTLING AND E. BECKER, *Comp. Meth. Appl. Mech. Engr.* **8** (1976), 51–60.
26. P. HOOD, *Int. J. Numer. Meth. Engr.* **10** (1976), 379–399.
27. S. TANEDA, *J. Phys. Soc. Japan* **46** (1979), 1935–1942.
28. R. SANI, P. GRESHO, D. TUERPE, AND R. LEE, Paper presented at the International Conference on Numerical Methods in Laminar and Turbulent Flow, University College of Swansea, Wales, July 17–21, 1978; also available as UCRL-80553, 1978.
29. R. LEE, P. GRESHO, AND R. SANI, *Int. J. Numer. Meth. Engr.* **14** (1979), 1785–1804.
30. R. L. LEE, P. M. GESHO, S. T. CHAN, AND R. L. SANI, *in* "Proceedings, Third International Conference on Finite Element Methods in Flow Problems, Banff, Alberta, Canada, June 10–13, 1980."
31. D. GARTLING, *Int. J. Numer. Meth. Engr.* **12** (1978), 187–190.
32. G. DE VAHL DAVIS AND G. MALLINSON, *Comput. Fluids* **4** (1976), 29–43.
33. A. MOULT, D. BURLEY, AND H. RAWSON, *Int. J. Numer. Engr.* **14** (1979), 11–35.
34. J. J. H. MILLER (Ed.), "Boundary and Interior Layers—Computational and Asymptotic Methods," Proceedings of BAIL 1 Conference held at Trinity College, Dublin, June 2–6, 1980, Boole Press Ltd., Dublin, Ireland, 1980.